SYNERGISTIC CORROSION INHIBITION OF ALUMINIUM-LITHIUM ALLOY

M Q ANSARI* and RAJPAL TYAGI

Department of Chemistry Multanimal Modi College Modinagar Ghaziabad India.

*Corresponding Author

Abstract: The nucleation and growth of the d phase is central to an understanding of the corrosion behaviour of these alloys. The Chemical composition of aluminium-lithium alloy (2091-T8), used in the present study was as follows: 1.8-2.5% Cu, 1.7-2.3% Li, 1.1-1.9% Mg, 0.3% Fe, 0.2% Si, 0.1% Cr, 0.1% Mn, 0.25% Zn, 0.1% Ti, 0.04-0.16% Zr and the remainder is Al. The density of the alloy was reported as 2.58 g/cm³.

Keywords: Synergistic Corrosion, Inhibition, Potentiostatic Polarisation

Introduction

Aluminium, as indicated by its position in the electromotive force (emf) series, is a thermodynamically reactive metal; among structural metals, only beryllium and magnesium are more reactive. Aluminium owes its excellent corrosion resistance and its usage as one of the primary metals of commerce to the barrier oxide film that is bonded strongly to its surface and that, if damaged, reforms immediately in most environments. This layer is attacked by alkaline solutions. On a surface freshly abraded and then exposed to air, the barrier oxide film is only 1 nm thick but is highly effective in protecting the aluminium from corrosion. The oxide film that develops in normal atmospheres grows to thickness much greater than 1 nm and is composed of two layers [1]. The inner oxide next to the metal is a compact amorphous barrier layer whose thickness is determined solely by the temperature of the environment. At any given temperature, the limiting barrier thickness is the same in oxygen, dry air, or moist air. Covering the barrier layer is a thicker, more permeable outer layer of hydrated oxide. Most of the interpretation of aluminium corrosion processes has been developed in terms of the chemical properties of these oxide layers. In addition to corrosion resistance, other properties of aluminium contributing to its widespread application are colourless and nontoxic corrosion products, appearance, electrical and thermal conductivity, reflectivity, and lightness or good strength-weight ratio. Pure aluminium is soft and weak, but it can be alloyed and heat- treated to a broad range of mechanical properties.

Aluminium alloys find application in engineering design chiefly on account of their light weight, high specific tenacity, resistance to corrosion or relatively low cost. Aluminium alloys are produced in a diversity of forms including castings, plate, sheet, shapes, forgings, bar, rod and wire. Both standard structural shapes and shapes of special design are commercial products. The tensile strength, yield strength, modulus of elasticity and hardness of aluminium alloys decrease with rising temperatures while the elongation increases. For most compositions the properties are greatly impaired at 400°F. But special alloys have been developed for satisfactory use at upwards

of 500°F. Aluminium alloys do not exhibit brittleness at low temperatures. In general, the strength, elongation and impact resistance improve with decreasing sub-zero temperatures. Aluminium shows excellent mechanical properties at cryogenic temperatures because it is a face- centred cubic material [2].

Lithium additions decrease the density and increase the elastic modulus of aluminium alloys, making aluminium-lithium alloys good candidates for replacing the existing high- strength alloys, primarily in aerospace applications. The realisation that addition of lithium to aluminium and its alloys can lead to very significant gains, has touched off world-wide activity. It has now become clear that lithium containing alloys of aluminium are promising alternatives to existing alloys [3]. Adding lithium to high strength aluminium alloys has been widely known as one of the main materials for aircraft part- members due to their attractive combination of low density, high specific elastic modulus and high specific strength, thus making them rather competitive to new non-metallic materials like carbon fibre reinforced composites. Because of the reactive nature of lithium, the corrosion behaviour of alloys containing lithium becomes necessary to be carefully examined [4].

One of the earliest aluminium alloys containing lithium was 2020. This alloy in the T6 temper was commercially introduced in 1957 as a structural alloy with good strength properties upto 175°C (350°F) [5]. It has a modulus 8% higher and a density 3% lower than alloy 7075-T6, but was rarely used in aircraft because of its relatively low fracture toughness. It was used in the thrust structure of the Saturn S-11, the second stage of the Saturn launch vehicle [6]. Three recently registered lithium- bearing alloys are 2090, 8090, and 2091. Alloy 2090, in T8-type tempers. Has a higher resistance to exfoliation than that of 7075-T6, and the resistance to SCC is comparable [7]. Alloy 8090 is being designed by various producers to meet other combinations of mechanical-property goals [8]. Although lithium is highly reactive, addition of up to 3% lithium to aluminium shifts the pitting potential of the solid solution only slightly in the anodic direction in 3.5% NaCl solution [9]. In an extensive corrosion investigation of several binary and ternary aluminium-lithium alloys, modifications to the microstructure that promote formation of the d phase (Al-Li) were found to reduce the corrosion resistance of the alloy in 3.5% NaCl solution [10]. It was concluded that an understanding of the nucleation and growth of the d phase is central to an understanding of the corrosion behaviour of these alloys. The Chemical composition of aluminium-lithium alloy (2091-T8), used in the present study was as follows: 1.8-2.5% Cu, 1.7-2.3% Li, 1.1-1.9% Mg, 0.3% Fe, 0.2% Si, 0.1% Cr, 0.1% Mn, 0.25% Zn, 0.1% Ti, 0.04-0.16% Zr and the remainder is Al. The density of the alloy was reported as 2.58 g/cm³.

Weight-loss Experiments

Square specimens (20 mm x 20 mm x 2 mm) of the aluminium- lithium alloy (2091-T8) were cut from the sheet. A small hole of 1.5 mm diameter was drilled near the upper edge in each specimen for mounting the specimen into the corrosive medium. The specimens were prepared, cleaned and evaluated as per ASTM GI-81 [11]. The specimens were grinded with 240-grit SiC (silicon carbide) paper and polished with 600-grit SiC paper until previous coarse scratches were removed. The edges were machined or polished to avoid preferential attack due to residual stresses from the cutting operation. The specimens were measured, washed in deionized water, degreased in AR grade acetone, air dried and weighed on an analytical balance to an accuracy of at least 1 mg.

The specimens were stored in a desiccator for a minimum of 24 hours before immersion. The surface area and mass of the test specimens were 9.00-10.00 cm² and 2.00-2.50 g respectively. The corrosive medium for the static immersion studies was 3% NaOH. The test solution was prepared by proper dissolution of AR grade sodium hydroxide [1310-73-2] in deionized water. The inhibitors used were of AR grade sodium silicate and barium chloride [10326-27-9]. The concentrations of inhibitors studied ranged from 0.10-0.40-gram percent each of sodium silicate and barium chloride. Each specimen (suspended with a nylon thread) was immersed in 500 ml covered beakers each containing 400 ml of test solution (3% NaOH) and proper amount of inhibitor(s) wherever required. Five specimens were used for each corrosive medium for studying the corrosion rate at five different time intervals. The testing periods were 48, 54, 60,66 and 72 hours. The temperature, throughout the experiment, was maintained at 30 ± 2°C. The specimens were cleaned by the following method after the test: The specimens were dipped in:

Nitric acid (HNO3, sp gr 1.42)	150 ml
Water to make	1 litre
Temperature	Room
Time	15 minutes or until clean

The extraneous deposits as well as bulky corrosion products were removed before the nitric acid treatment to avoid violent reactions that may result in attack of the sound metal. The specimens were washed with deionized water, air dried and weighed to an accuracy of atheist ±1 mg. The mass lost during the test were determined and corrosion rate in mils per year (mpy) was calculated as per ASTM G31-72 [11] from the following expression:

$$R = \frac{KW}{ATD}$$

Where:

R = corrosion rate in mpy.

K = a constant, valued 3.45×106,

W = mass loss in g to the nearest 1 mg,

A = area in cm² to the nearest 0.01 cm².

T= time of exposure in hours to the nearest 0.01 hr, and

D= density in g/cm³

The value of percent inhibition efficiency was calculated from the following relation:

$$\eta = \frac{R_u - R_f}{R_u} \times 100$$

Where, R_u, and R_f, are the corrosion rates in the absence and in the presence of inhibitor(s) respectively. To observe the synergistic effect of corrosion inhibitors, the corrosion rate was determined in different concentrations of one inhibitor keeping the concentration of another inhibitor constant and vice versa. But to avoid the lengthening of manuscript, only the best synergistic combination of corrosion inhibitors has been reported.

Potentiostatic Polarisation Measurements

For polarisation studies, rectangular specimens (20 mm × 10 mm x 1.5 mm) with a narrow strip (15 mm x 3 mm × 1.5 mm) at one end were cut from the sheet of aluminium-lithium alloy (2091-T8). Within one hour of the experiment the working electrodes (test-specimens) were prepared. Wet grinding with 240-grit Sic (silicon carbide) paper was followed by wet polishing with 600-grit SiC (silicon carbide) paper until previous coarse scratches were removed, was performed. The test specimens were rinsed and dried. Each working electrode (test specimen) was drilled, tapped and mounted onto the electrode holder. The back and sides of the working electrode were coated with a mixture of Perspex and wax from chloroform solution, leaving only the 1 cm² portion of the working electrode exposed to the test solution (3% NaOH). The volume of the test solution was 300 ml in the polarisation cell (corrosion cell). The auxiliary electrode (platinum electrode), salt- bridge probe and other components were placed in the test cell (corrosion cell) and the salt-bridge was filled with the test solution (3% NaOH). The working electrode was transferred to the test cell and the salt-bridge probe tip was adjusted in the manner that it was about 2 mm away from the test specimen. The open-circuit potential Ecorr (corrosion potential) of the test specimen after 5 and 55 min immersion was recorded and Ecorr was suppressed. After this the potentiostatic potential scan was started at a constant step rate of 10 mV/min and the corresponding current densities were recorded.

These steps were repeated until a potential of 350 mV vs SCE more active than corrosion potential was achieved. The cathodic polarisation scan was performed first and after one minute the anodic polarisation scan was performed. The polarisation curve was plotted as a linear potential-current density curve and the cathodic and anodic potentiostatic polarisation data were plotted on a semilogarithmic paper in accordance with practice G3-74 [11], (potential-ordinate, current density-abscissa). The polarisation resistance, R, was determined graphically as the tangent of the linear polarisation curve at the origin of the plot (AE= 0), and babe (anodic and cathodic Tafel slopes) were obtained from E vs log I graph (Tafel plots or Evan's diagram). Each step was performed as per ASTM G3-74, G5-87 and G59-78 [11]. The corrosion current density I_{corr} was calculated from the following equation:

$$I_{corr} = \frac{b_a b_c}{2.303(b_a + b_c)R_p}$$

Where:

I_{corr} = corrosion current density in A/cm²,

b_a = anodic Tafel constant in Volts/Decade of current,

b_c = cathodic Tafel constant in Volts/Decade of current,

R_p polarisation resistance in ohm.cm², and

2.303 = the natural log of 10.

The corrosion current density I_{corr} has also been evaluated from the intersection of the extrapolated anodic and cathodic Tafel plots in the Evan's diagram.

Results and Discussions

Weight-loss Kinetics

The corrosion rate of Al-Li alloy is very high in 3% NaOH solution which increases with time to reach a maximum and then decreases continuously. Corrosion of Al- Li alloy in 3% NaOH is very much inhibited in presence of small concentrations of Sodium silicate. Presence of 0.10% sodium silicate reduces the corrosion rate to more than half and this further decreases as the silicate concentration is increased till it reaches a minimum (approx. 253-270 mpy) at 0.25% sodium silicate concentration. Surprisingly, a further increase in concentration of sodium silicate from 0.25% to 0.30% results in a sudden increase in corrosion rate to almost double. The corrosion rate with 0.35% Na_2SiO_3 is further increased and this is almost double of rate at 48 hours, about four times at 54 and 60 hours and the rate also decrease with time. It tends to be uniform at 0.40% Na_2SiO_3 concentration showing that it has reached a maximum value which is much higher than in 3% NaOH alone. Thus, a reactivation of corrosion processes is evident. It is evident that percent inhibition efficiency of sodium silicate is maximum around 60 hours with 0.10% Na_2SiO_3 but an increase in concentration of sodium silicate from 0.15% to 0.25% gives maximum percent inhibition efficiency around 54 hours and the highest
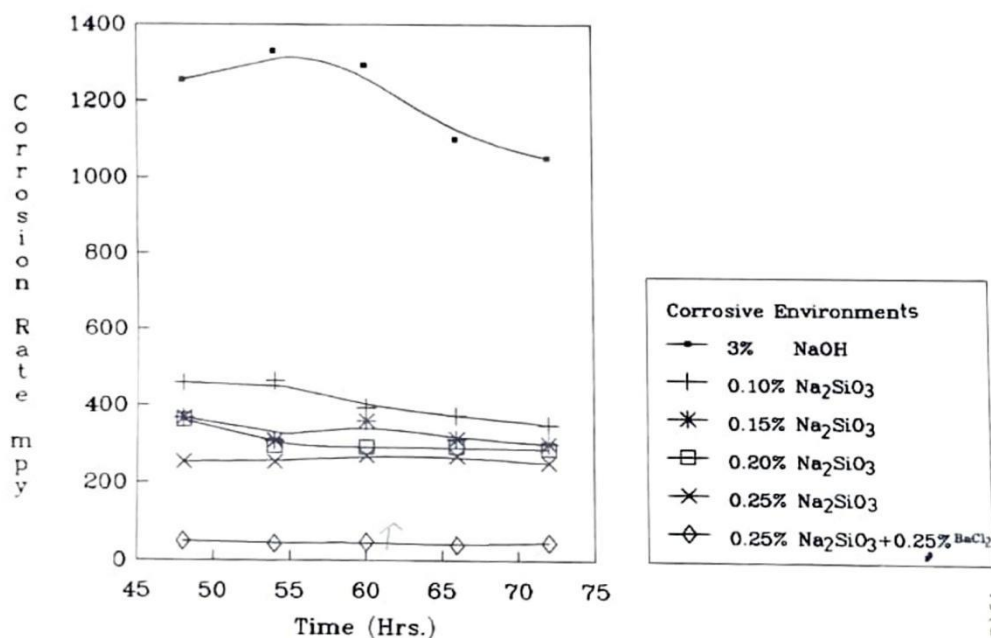
Figure 1. Corrosion studied (Corrosion rate) of Al-Li Alloy Sodium Silicate-Barium Chloride in 3% NaOH.

efficiency is 80% with 0.25% Na_2SiO_3. This value is much less than the percent inhibition efficiency obtained with synergistic combination of sodium silicate and barium chloride (96% approx.), it is also obvious that the corrosion rate generally decreases with time when uninhibited but shows a maximum corrosion rate at 54 hours which decreases with time. Thus, an initial inhibition is indicated in such cases while initial corrosion rates (after 48 hours) are higher when corrosion is inhibited and these also decrease with time. The corrosion rate in presence of 3% NaOH alone and synergistic combination of sodium silicate and barium chloride are also given in the table and figures for the sake of comparison. A sharp decrease in corrosion rate is P observed with 0.10% $BaCl_2$ and again the inhibiting action of barium chloride increase with increase in concentration of this electrolyte showing maximum inhibition at 0.25% $BaCl_2$. The corrosion rate increases with 0.30% BaCl2 and then suddenly shows an approximately three times increase in corrosion rate with 0.35% $BaCl_2$. The corrosion rate with 0.35% and 0.40% $BaCl_2$ is more than the corrosion rate of the Al-Li alloy with 3% NaOH solution alone. This is again unusual as observed with sodium silicate.

CORROSION STUDIES OF Al—Li ALLOY (2091—T8)
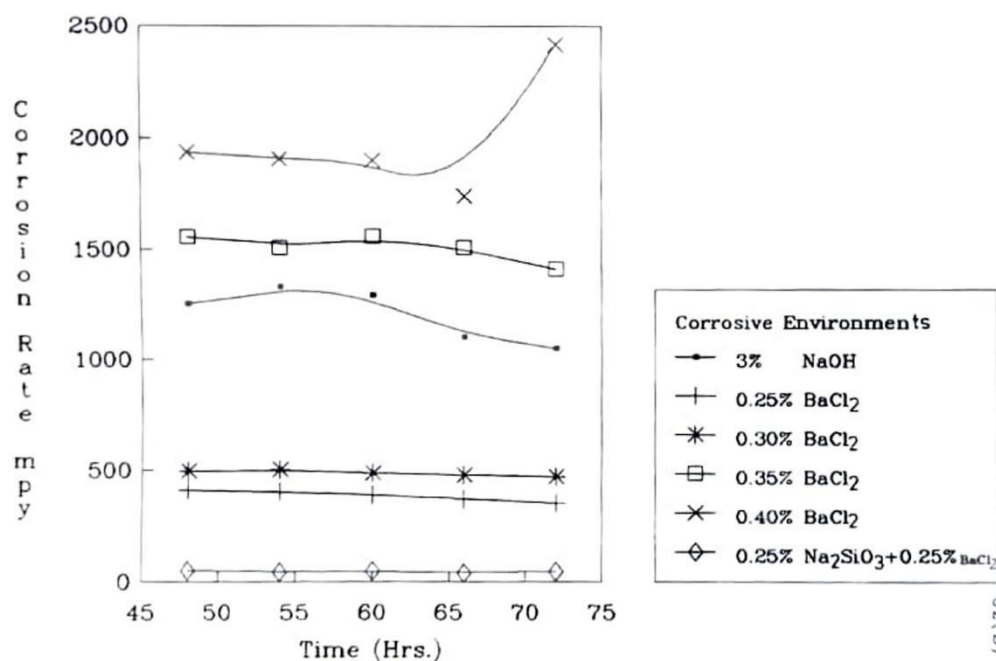Sodium silicate—Barium chloride in 3% NaOH

Figure 2. Corrosion studied (Corrosion rate) of Al-Li Alloy Sodium Silicate-Barium Chloride in 3% NaOH.

Potentiostatic Polarisation Studies

Corrosion current densities I_{corr} have been determined by linear polarisation and Tafel extrapolation methods. The values of E_{corr} calculated I_{corr} from Linear Polarisation method and evaluated by extrapolation method (Evan's diagram) in presence of corrosive alkaline medium with and without inhibitors. The values of linear polarisation resistance R_p, anodic Tafel slope b, and cathodic Tafel slope b, for each solution are also given along with each set of figures. It is easily understood that E_{corr} shifts towards less negative values in presence of 0.25% sodium silicate or 0.25% barium chloride in 3% NaOH solution when the corrosion rate is minimum with each inhibitor/electrolyte separately, as seen earlier with weight-loss study. E_{corr} of the alloy continues to shift towards less negative values or anodic direction as the concentration of barium chloride is increased in sodium hydroxide solution with 0.25% sodium silicate. The maximum shift occurs when the barium chloride concentration is also 0.25% and the corrosion current density I_{corr} is minimum i.e., 8.10×10 A/cm^2 by linear polarisation method and 6.00×10" A/cm by Tafel extrapolation method. A slight increase in concentration of barium chloride i.e., from 0.25% to 0.30% shifts E_{corr} to a higher negative value and I_{corr} also registers a large increase in its value.

CORROSION STUDIES OF Al-Li ALLOY (2091-T8)
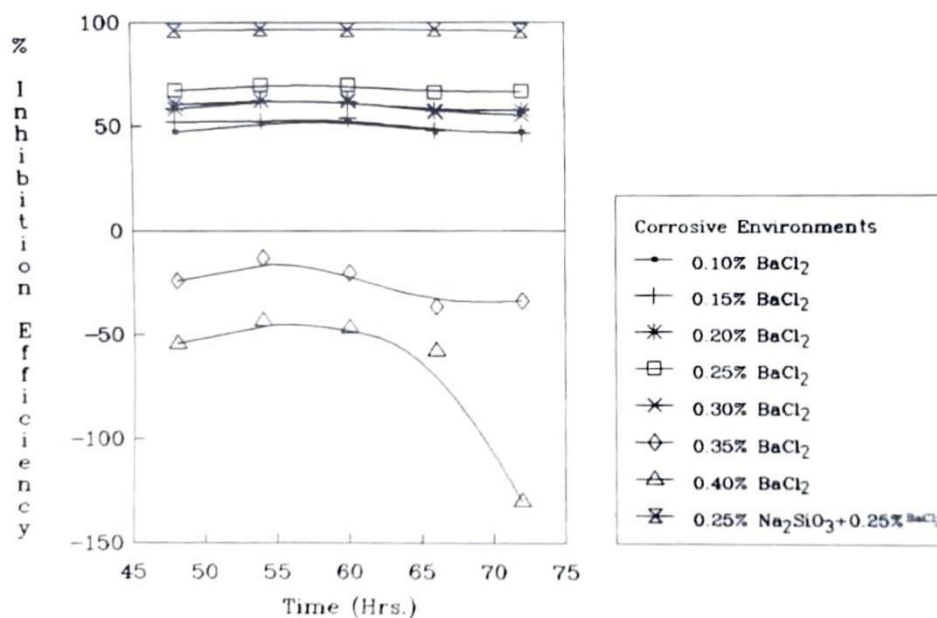Sodium silicate-Barium chloride in 3% NaOH

Figure 2. Corrosion studied (Inhibition Efficiency) of Al-Li Alloy Sodium Silicate-Barium Chloride in 3% NaOH.

Further increase in concentration to 0.35% again $BaCl_2$ almost doubles the I_{corr} though a very slight change is seen in the value of E_{corr}. These results indicate that both anodic and cathodic reactions are reactivated simultaneously as E_{corr} value has not changed with 0.25% $BaCl_2$, the shift in E_{corr} of the alloy in 3% NaOH is approximately 165 mV to 195 mV towards less negative or anodic direction which is much less than the shift observed with 0.25% sodium silicate in 3% NaOH (205 mV-230 mV). Accordingly, the corrosion current density I_{corr} is higher or inhibition efficiency is less with 0.25% $BaCl_2$ as compared to 0.25% Na_2SiO_3. Addition of sodium silicate to corrosive solution of 3% NaOH + 0.25% $BaCl_2$, further shifts the Ecorr values towards anodic direction though to lesser extent as compared to changes in Ecorr on addition of $BaCl_2$ to the solution of 3% NaOH+0.25% sodium silicate (7 mV-18 mV) as compared to 20 mV-25 mV in the previous experiment. There is again a jump in Ecorr values at synergistic combination of 0.25% $BaCl_2$ +0.25% Na_2SiO_3 reaching -980 mV to -1010 mV when the corrosion current density is minimum. The Ecorr value again shifts towards more negative value when the concentration of sodium silicate is increased to 0.30% and I_{corr} is higher. A further increase in sodium silicate concentration i.e., 0.35% surprisingly, does not show expected change in the E_{corr} value or the corrosion current density.
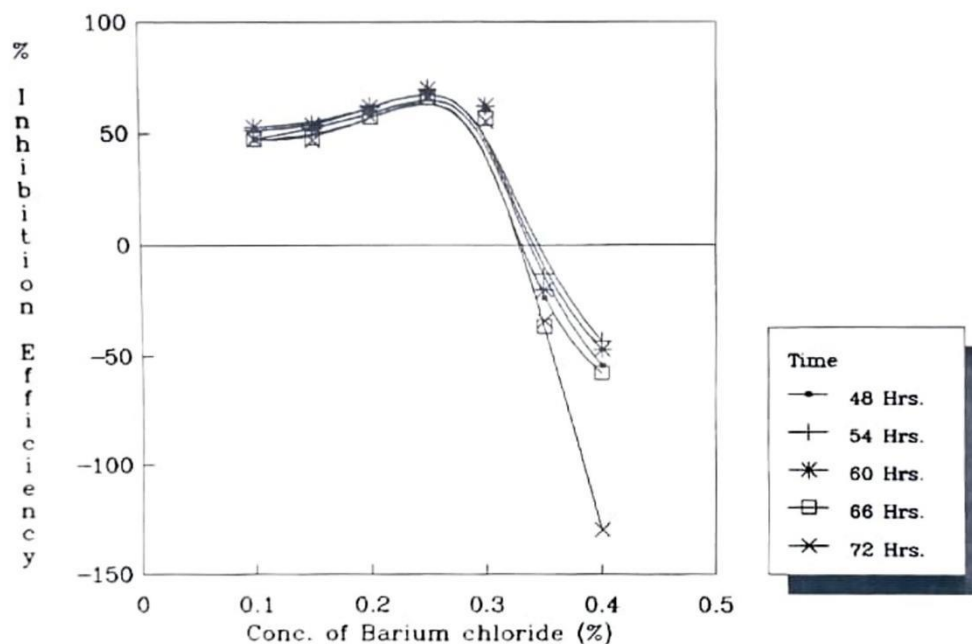
Figure 2. Corrosion studied (Inhibition Efficiency) of Al-Li Alloy Sodium Silicate-Barium Chloride in 3% NaOH.

Conclusion

The results of this study also indicate that a complete protection of the alloy is not possible with either inhibitor or with the synergistic combination but corrosion can be reduced to a great extent with this synergistic combination. A further study of the corrosion process in 3% NaOH solution with 0.25% sodium silicate, 0.25% barium chloride and different combinations of inhibitors concentrations were undertaken by electrochemical methods for better understanding of the mechanism of inhibition and synergistic effects. The results of the investigations by weight-loss method and electrochemical studies shows that corrosion rate of Al-Li alloy in 3% NaOH solution is very high and it is inhibited by both sodium silicate and barium chloride. Percent inhibition efficiency of Na_2SiO_3 is higher than $BaCl_2$. Both Na_2SiO_3 and $BaCl_2$ show acceleration in corrosion rate beyond 0.25% concentration in 3% NaOH. The corrosion rate at higher concentration of both the inhibitors is much higher than corrosion rate in the absence of these inhibitors. Both the inhibitors show synergistic effect at some concentration and the highest percent inhibition efficiency is shown by a combination of 0.25% each in 3% NaOH solution.

Acknowledgement

References

1. Hunter, M. S., Fowle, P. J. Electrochem. Soc. 103 (1956) p. 482.

2. Fontana, M. G: Greene, N. D. Corrosion Engineering 2nd ed., p. 170 McGraw-Hill International Book Company, 1978.

3. Shreie, L. L Corrasion Vol 1, 2nd ed. Hewnes-Butterworths, 1978.

4. Logan, H. L. The Stress Corrasion of Metals Wiley, New York, 1966.

5. Robertson, W. D. Stress Corrosion Cracking and Embrittlement Wiley, New York, 1956.

6. Burton, C. L; Mayer, L. W.; Spuhler, E. H. Aircraft and Aerospace Applications, in Aluminium, Vol II, K. R. Van Horn, Ed. American Society for Metals, 1967.

7. Bretz, P. E.; Sawtell, R. R. The Institute of Metals (1986) p. 47 Alithilite Alloys: Progress, Products and Properties Proceedings of the Third Aluminium- Lithium Conference.

8. Peel, C. J.; Evans, B.; McDarmaid, D. Proceedings of the Third Aluminium-Lithium Conference (1986) p. 26.

9. DeJong, H. F.; Martens, J. H. M. Aluminium 61 (1985) 6, p. 416.

10. Niskanen, P. Sanders, Jr., T. HA Rinker, J. G., Marek, M. Corrosion Science 22 (1982) 4, p. 283.

11. Metal Corrosion, Erosion, and Wear Annual Book of ASTM Standards Vol 03.02 American Society for Testing and Materials, 1987.